Exosomes from M2 macrophages promoted glycolysis in FaDu cells by inhibiting PDLIM2 expression to stabilize PFKL

Peng WANG[1], Guang-Yao LI[1], Lei ZHOU[1], Huai-Li JIANG[1], Yue YANG[2], Hai-Tao WU[2,*]

[1]Department of Otorhinolaryngology, Head and Neck Surgery, Zhongshan Hospital, Fudan University, Shanghai, China; [2]ENT institute and Department of Otorhinolaryngology, Eye & ENT Hospital, Fudan University, Shanghai, China

*Correspondence: eentwuhaitao@163.com

Laryngeal squamous cell carcinoma (LSCC) is one of the most prevalent malignant diseases worldwide. LSCC patients suffer from a severe decline in life quality, due to the essential roles of the larynx in basic functions in the human body. The overarching goal of the present study is to explore whether exosome from M2 macrophages promotes LSCC by targeting glycolysis. In the current study, the expression of PDLIM2, an E3 ubiquitin ligase, in clinical samples was monitored by quantitative PCR and immunohistochemical examination. Extracellular acidification rate (ECAR) and oxygen consumption rate (OCR) were measured by the Seahorse machine. Cell proliferation was measured by using Cell Counting Kit-8. A luciferase assay was performed to verify the regulation of miRNA on its target gene. The results showed that PDLIM2 exhibited downregulation in LSCC clinical samples and was associated with stage and differentiation of tumors in patients. In FaDu cell line, PDLIM2 inhibited cell proliferation and glycolysis but promoted the ubiquitination of PFKL. Exosomes from M2-type macrophages delivered miR-222-3p into LSCC cells to suppress PDLIM2 expression, leading to the elevated expression of PFKL and enhanced glycolysis which accelerated the proliferation of FaDu cells. The findings from cultured cells were supported by a subcutaneous tumor growth model in nude mice. Collectively, our data provided a snapshot of the miR-222-3p/PDLIM2/PFKL axis in LSCC tumorigenesis, and in concert with the importance of TAM exosomes and glycolysis, could be potentially translated to LSCC clinics.

Key words: aerobic glycolysis, exosome, laryngeal squamous cell carcinoma, tumor-associated macrophage

Counting for about 25% of total cases of head and neck squamous cell carcinoma (HNSCC), laryngeal squamous cell carcinoma (LSCC) is one of the most prevalent malignant diseases with an annual incidence rate of 2.4% globally [1, 2]. Regarding the essential roles of the larynx in basic functions in the human body, including vocalization, breathing, and swallowing, LSCC always causes a severe decline in the quality of daily life for patients [3]. Despite the application of advanced levels of radiotherapy, chemotherapy, and surgical intervention, it is still difficult to cure the LSCC with advanced stage, as evidenced by the fact that the long-term survival rate remains at 50%, considered the highest mortality in various kinds of HNSCC [4]. Hence a detailed understanding of molecular mechanisms of LSCC that could direct future therapeutic development is still a pressing requirement.

Metabolic reprogramming is a biochemical hallmark of cancers [5]. Compared with normal cells, cancer cells always exhibit preferential dependence on glycolysis for energy production in an oxygen-independent manner, which is considered a critical factor to promote tumorigenesis. Accumulating evidence indicated that glycolysis is associated with the progress of LSCC tumors. Among the key enzymes involved in glycolysis, phosphofructokinase (PFK) is the most essential rate-limiting one. PFK is expressed with three different isoforms in human bodies: PFKL (liver), PFKM (muscle), and PFKP (platelet) [6]. PFKL was shown to be targeted by A20 E3 ubiquitin ligase in hepatocellular carcinoma (HCC) that promoted glycolysis and tumorigenesis [7]. Hence PFKL becomes an inviting focus of LSCC study to examine if PFKL is regulated by E3 ubiquitin ligase for the protein degradation and therefore contributes to abnormal glycolysis in LSCC cells.

The microenvironment of most solid tumors consists of up to 50% macrophages, defined as tumor-associated macrophages (TAMs), which are recruited into the tumor microenvironment under the specific stimulation. The biological activity of TAMs in tumorigenesis has received much recent

attention [8]. These macrophages (M0) could develop into two major categories, known as M1 and M2. M1 always represents the classically activated macrophages, while the M2 is considered as alternatively activated macrophages. M2 macrophages do not function to clear tumor cells, but alternatively to facilitate the tumor cells to escape from immune clearance and spread to other parts of the human body [8]. It was reported that TAMs residing in the LSCC microenvironment were associated with disease prognosis and induced M2 differentiation [9, 10].

Cells, including macrophages, produce and secret small cell vesicles with diameters measured between 30 and 150 nm, called exosomes, for the exchange of material with other cells [11]. In tumors, exosomes actively participate in the communication between cancer cells and tumor niche cells that influence the survival, growth, and metastasis of tumors [12]. TAMs with M2-polarization enable tumorigenesis of multiple types of cancers through secreting exosomes (for example, gastric cancer [13], pancreatic cancer [14], breast cancer [15], colon cancer [16]). These exosomes deliver a large amount of miRNA, lncRNA, and specific proteins to cancer cells and enable their growth and metastases to distant tissues [12]. These observations beg the question that whether LSCC also contains TAMs with a tumor-promoting role and whether exosomes are involved in the mechanisms of proliferation and glycolysis.

Motivated by previous reports described above, the overarching goal of the present study is to explore whether exosomes from M2 macrophages promote LSCC by targeting glycolysis. In particular, the involvement of E3 ubiquitin ligase and its putative substrate, PFKL, would be extensively studied. PDLIM2, an E3 ubiquitin ligase and PDZ and LIM domains-containing protein family member, exhibited the downregulation in LSCC and acted as a tumor-suppressor in LSCC cells by promoting degradation of PFKL enzyme and therefore, inhibiting glycolysis and proliferation of the cells. The exosomes from LSCC-associated M2-type macrophages delivered miR-222-3p into LSCC cells to suppress PDLIM2 expression and enhance glycolysis and tumorigenesis of LSCC. These findings consistently from cultured cells and animal models provide a snapshot of the miR-222-3p/PDLIM2/PFKL axis in LSCC tumorigenesis, and in concert with the importance of TAM exosomes and glycolysis, could be potentially translated to LSCC clinics.

Materials and methods

Chemicals and cell lines. GW4869 and MG132 were purchased from Sigma-Aldrich (LAA21, St. Louis, MO, USA). Human monocyte, THP-1 cell line was purchased from the cell bank of Shanghai Biology Institute, Chinese Academy of Science (Shanghai, China). THP-1 cells were cultured in PRMI-1640 medium, and FaDu cells (a cell line originating from human pharyngeal squamous cell carcinoma) and human HEK-293 cells were cultured in DMEM medium, both with 10% FBS (Gibco) addition. The incubator was set at 37 °C and the flowed air contained 5% CO_2.

THP-1 cells were induced to differentiate. The condition: 100 ng/ml phorbol-12-myristate-13-acetate (from Millipore Sigma). The culture medium was changed every two days a week. After differentiation, the cells were treated with 30 ng/ml of IL-4 (Biolegend) for about 24 h longer, then washed and placed into a fresh medium.

Manipulating PDLIM2 and miR-222-3p in cells. Short hairpin RNA (shRNA) oligos targeting PDLIM2 (sh-1, 5'-GCCCATCATGGTGACTAAG-3'; sh-2, 5'-GAGAGT-CAGTCCTCCTTAA-3') were annealed and cloned into pLKO.1 (Addgene, Cambridge, MA, USA). The full-length human PDLIM2 was cloned into pLVX-puro (Clontech, Palo Alto, CA, USA). The lentivirus of shPDLIM2, control shRNA (shNC), pLVX-PDLIM2 (oePDLIM2), or pLVX-puro (Vector) was packaged in 293T cells along with packaging plasmids, psPAX2 and pMD2.G. The target cells were infected with the lentivirus and selected by the corresponding agents.

The target cells were also transfected by using Lipofectamine 2000 reagent (ThermoFisher) for miR-222-3p mimic (50 nM, 5'-AGCUACAUCUGGCUACUGGGU-3'), inhibitor (50 nM, 5'-ACCCAGUAGCCAGAUGUAGCU-3'), or also the negative control miRNA (50 nM, 5'-CAGUA-CUUUUGUGUAGUACAA-3').

Human laryngeal squamous cell cancer (LSCC) sample collection. The present investigation was under the management according to our hospital's ethical guideline which was updated by our Institutional Ethical Review Committee. LSCC tissues and their corresponding adjacent non-tumorous tissues were obtained from patients receiving surgery from 2019 to 2020 at Zhongshan Hospital, Fudan University (Shanghai, China), with written informed consent signed. Related clinical information was obtained by a review of the medical records of the patients.

Real-time quantitative PCR (qPCR). Total messenger RNA was extracted from cells with TRIzol reagent (Thermo-Fisher), based on the manufacturer's recommended protocol. The mRNA was then reverse-transcribed to produce cDNA using Revert-Aid™ Kit (ThermoFisher). For miRNA experiments, a pair of specially-designed stem-loop primers were used, and the random primers were used for mRNA transcripts. The quantitative real-time PCR reactions were carried out with SYBR Green PCR Master Mix (Thermo-Fisher), taking GAPDH as an internal control for normalization. The primers used in this study could be found in Supplementary Table S1 and Supplementary Table S2. The qPCR was conducted on the 7300 Real-time PCR System (Applied Biosystems, USA).

Immunohistochemistry (IHC) analysis. The pathological tumor and control samples were fixed by formalin, sectioned, and embedded with paraffin for storage. After removing paraffin in xylene and then re-hydration in absolute EtOH, these sections were processed for antigen retrieving with microwave heating in citrate buffer (0.01 M with pH 6.0) for

15 min. The endogenous peroxidases in sections were then inactivated by 0.3% hydrogen peroxide for 30 min treatment. The sections were then treated with 10% normal goat serum, which requires about 30 min for blocking non-specific antigens. Following incubation with primary antibody against PDLIM2 (Abcam, ab246868) at 4 °C for 16 h, the sample slices were further incubated with a secondary antibody with conjugation of horseradish peroxidase (HRP) for 1 h at RT. Immunoreactive signals in slides were revealed by 3,3-diaminobenzidine (DAB) solution (Vector Laboratories, Burlingame, CA, USA) and counterstaining was conducted with hematoxylin. The intensity of immunoreactivity was classified independently by two researchers as follows: Staining index = staining intensity (SI) × percentage of positive cells. The SI was defined as 0, negative; 1, weak; 2, moderate; 3, strong. A staining index of 3 was set as the threshold for PDLIM2 low expression and high expression.

Western blotting. Lysate of whole cells was quickly generated in a pre-cold RIPA buffer. The lysate of total protein was measured for concentration using the BCA kit (Thermo-Fisher) with the protocol provided by the manufacturers. The protein extract was resolved on the 10–15% SDS-PAGE gel and transferred and electro-blotted onto the nitrocellulose membrane (Millipore). Membrane with transient wash was then blocked by incubation with 5% non-fat milk and then primary antibodies were added (listed in Table S3) at 4 °C for 16 h. The secondary antibodies with conjugation of horseradish peroxidase (Cell Signaling) were used for chemiluminescent signal determination. Immunoreactive signals were revealed by a kit of ECL chromogenic substrates (Bio-Rad).

Cell proliferation assay. Cell proliferation was assessed by using Cell Counting Kit-8 (Dojindo Laboratories, Japan) according to the manual from the manufacturer. The optical densities (OD) absorbance was measured at 450 nm.

Experiments of cellular energy metabolism. The oxygen consumption rate (OCR) and extracellular acidification rate (ECAR) were measured with an XF96 analyzer (Seahorse Bioscience) and the manipulation strictly followed the manual from the manufacturer. For ECAR, the Glyco-stress test kit (Seahorse Bioscience), 10 mM glucose, 50 mM 2-[N-(7-nitrobenz-2-oxa-1,3-diazol-4-yl)amino]-2-deoxyglucose, and 2 μM oligomycin were included. For OCR, the Mito-stress kit (Seahorse Bioscience), 1.5 μM FCCP [carbonyl cyanide 4-(trifluoromethoxy) phenylhydrazone], 2 μM oligomycin, and 1 μM antimycin A with 100 nM rotenone were included.

Co-immunoprecipitation (co-IP). Freshly prepared whole cell lysate in co-IP buffer (Tween-20) was immunoprecipitated with the following antibodies: anti-PDLIM2 (Abcam, ab246868), anti-PFKL (Abcam, ab241093), or control IgG (Santa Cruz Biotech., Santa Cruz, CA, USA), and with agarose beads with protein A or protein G at 4 °C for 16 h (or over-night). Precipitates from this step were washed by cold co-IP buffer three times and then subjected to western blot detection to examine the pull-down efficacy.

Exosome isolation. The medium from cultured cells was centrifuged and the pellet (mainly cell debris) was removed. Then the supernatant was further cleaned by 0.22 μm PVDF membrane filter. Exosomes were extracted from this material using high-purity and high-efficient VEX Reagent (Vazyme, Nanjing, China) according to the manufacturer's manual. Exosomes were resolved in PBS and frozen at –80 °C for future analysis. The protein abundance level of TSG101 and CD63 was determined by western blot.

Exosomes uptake assay. PKH-26 was used to specifically label exosomes with Red Fluorescent Cell Linker Kits (Sigma-Aldrich). The signal was visualized as the exosomes were uptaken by target cells. Briefly, exosomes were initially diluted with the kit's component Diluent C, and then carefully incubated with PKH-26 red fluorescent dye at 25 °C for 5 min. Next, the sterile FBS was added and then the mixture was left for 1 min more for sufficient staining. Then, the staining product was transferred and extensively washed by KSFM and centrifuged at the highest speed at 4 °C for about 75 min. The labeled exosomes remain at the bottom of tubes after discarding upper layer supernatant and were then resuspended by KSFM. 1 mg of labeled exosomes was added into cultured FaDu cells on a round coverslip in a 24-well plate, and then incubated in a standard condition (5% CO_2, 37 °C) for 16 hours or overnight. Later, the cells were washed twice with PBS and then fixed for 10 min by 4% PFA. The slides were then mounted with an anti-fluorescent-quenching agent, together with DAPI.

Luciferase assay. 3'-UTR segment (WT or mutant) from the PDLIM2 gene was integrated into the vector pGL3 (Promega, Madison, WI, USA). The negative control or miR-222-3p mimic was introduced into FaDu cells by transient transfection, together with plasmids of WT or mutant pGL3-PDLIM2-3'-UTR (using Lipofectamine 2000 reagent for transfection). Luciferase activity was monitored with a luciferase assay kit (Promega) with a luminometer. The signals were normalized by a concentration of lysate protein, and further normalized by pGL3-transfected control samples.

Tumor growth in mice. All described mice experiments were performed with protocols provided by the Institutional Animal Care and Use Committee of Zhongshan Hospital (Shanghai, China). Briefly, FaDu cells (control, or with stable expression of PDLIM2, named oePDLIM2) were subcutaneously injected into 6–8-week-old nude mice (female, athymic, from Shanghai Laboratory Animal Center). Xenograft tumors were formed slowly. Seven days after injection, mice were randomly assigned into the four groups (each group had 5 mice), then injected with exosomes produced from M2-macrophages every 3 days. Tumor growth was monitored every day and the size of tumors was measured by digital calipers every three days (calculation: volume = 0.5 × length × width^2). The mice were sacrificed at about 33 days after injection and the tumor weight was measured.

Statistical analysis. Data analysis with statistics was conducted in the software of GraphPad Prism (version 6.0, San Diego, CA, USA). p-values were calculated by ANOVA or unpaired Student's t-test.

Results

Downregulation of PDLIM2 expression in LSCC tumors. As the evidence is accumulated to indicate the broad involvement of PDLIM2 in the pathogenesis of malignant diseases [17], we attempted to evaluate the association of PDLIM2 expression with LSCC. Samples from 25 pairs of LSCC and control subjects were used to monitor the mRNA

expression of PDLIM2 by qPCR. PDLIM2 mRNA showed a strong reduction in LSCC samples (Figure 1A). Immunohistochemical examination for the protein expression level of PDLIM2 in tumor slice samples categorized LSCC patients into two types: PDLIM2-high and PDLIM2-low (Figure 1B). To analyze the clinical data of these 2 categories of patients, we found that patients in the PDLIM2-low group displayed a lower level of cell differentiation and more advanced stage, though the primary location and lymphatic metastasis of the tumors were comparable in these 2 categories (Table 1). These findings implicate the mechanistic involvement of PDLIM2 in the pathogenesis of this tumor.

PDLIM2 inhibits proliferation and aerobic glycolysis in FaDu cells. Aiming to examine the effects of PDLIM2 on tumorigenesis of LSCC cells, the LSCC cell line, FaDu, was stably transfected to overexpress PDLIM2, which was confirmed by the western blot (Figure 2A). Compared with FaDu cells with control transfection, PDLIM2-overexpressing FaDu cells exhibited significant suppression of proliferation, indicated by the CCK-8 assay (Figure 2B). To determine the effects of PDLIM2 on mitochondrial metabolism, the critical factor influencing tumorigenesis of LSCC, the control and PDLIM2-overexpressing FaDu cells were tested with Seahorse XF analyzers. ECAR analysis indicated that glycolysis in FaDu cells was significantly inhibited by PDLIM2 overexpression (Figure 2C). Consistently, the OCR analysis also showed reduced oxidative phosphorylation in PDLIM2-overexpressing FaDu cells (Figure 2D).

In parallel with PDLIM2-overexpressing cells, we also generated FaDu cells with the expression of shRNA targeting PDLIM2. After confirming the knock-down efficiency (Figure 2E), the proliferation and mitochondrial metabolism were examined in these cells. CCK-8 assay revealed that PDLIM2 knock-down significantly promoted proliferation (Figure 2F). Seahorse ECAR (Figure 2G) and OCR (Figure 2H) analysis indicated enhanced glycolysis and oxidative phosphorylation, respectively, in PDLIM2 knock-down cells. These findings support the notion that PDLIM2
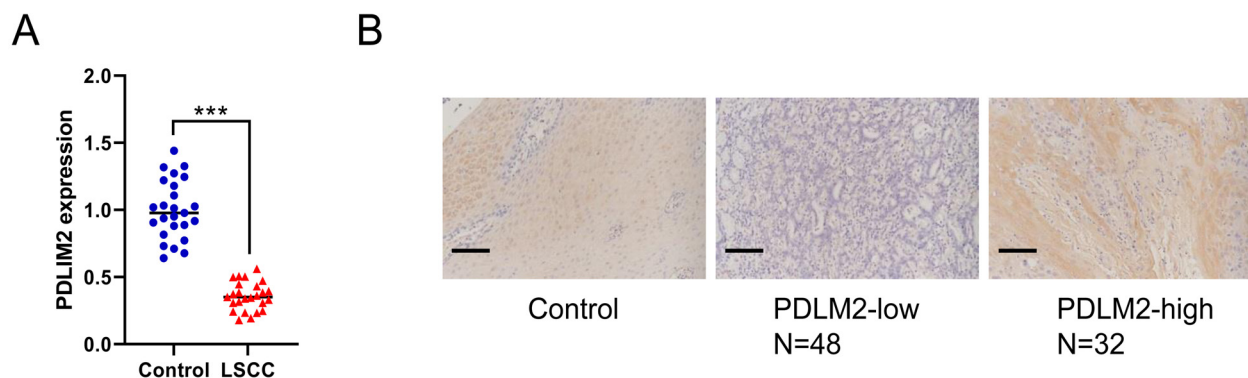
Table 1. Correlation between PDLIM2 expression and clinicopathologic factors of LSCC patients.

Variables	All cases	PDLIM2 protein		p-value
		High (n=32)	Low (n=48)	
Age				
≤60	33	14	19	0.8176
>60	47	18	29	
Gender				
Male	75	32	43	0.6488
Female	5	3	2	
Primary location				
Supraglottic	3	2	1	0.5752
Glottis	56	21	35	
Subglottic	21	9	12	
Differentiation				
Well and moderate	50	25	25	0.0206*
Poor	30	7	23	
Lymphatic metastasis				
Absent	46	17	29	0.6450
Present	34	15	19	
Clinical stage				
I–II	36	20	16	0.0126*
III–IV	44	12	32	

*p<0.05 by Fisher's exact test

Figure 1. Downregulation of PDLIM2 expression in LSCC tumors. A) qPCR examination showed a reduced level of PDLIM2 mRNA in LSCC samples compared with samples from 25 paired control subjects. Data presented as mean ± S.D., ***p<0.001 (unpaired Student's t-test). **B)** Immunohistochemical staining for PDLIM2 in pathological slice samples from LSCC patients and control subjects. Scale bar: 50 mm.
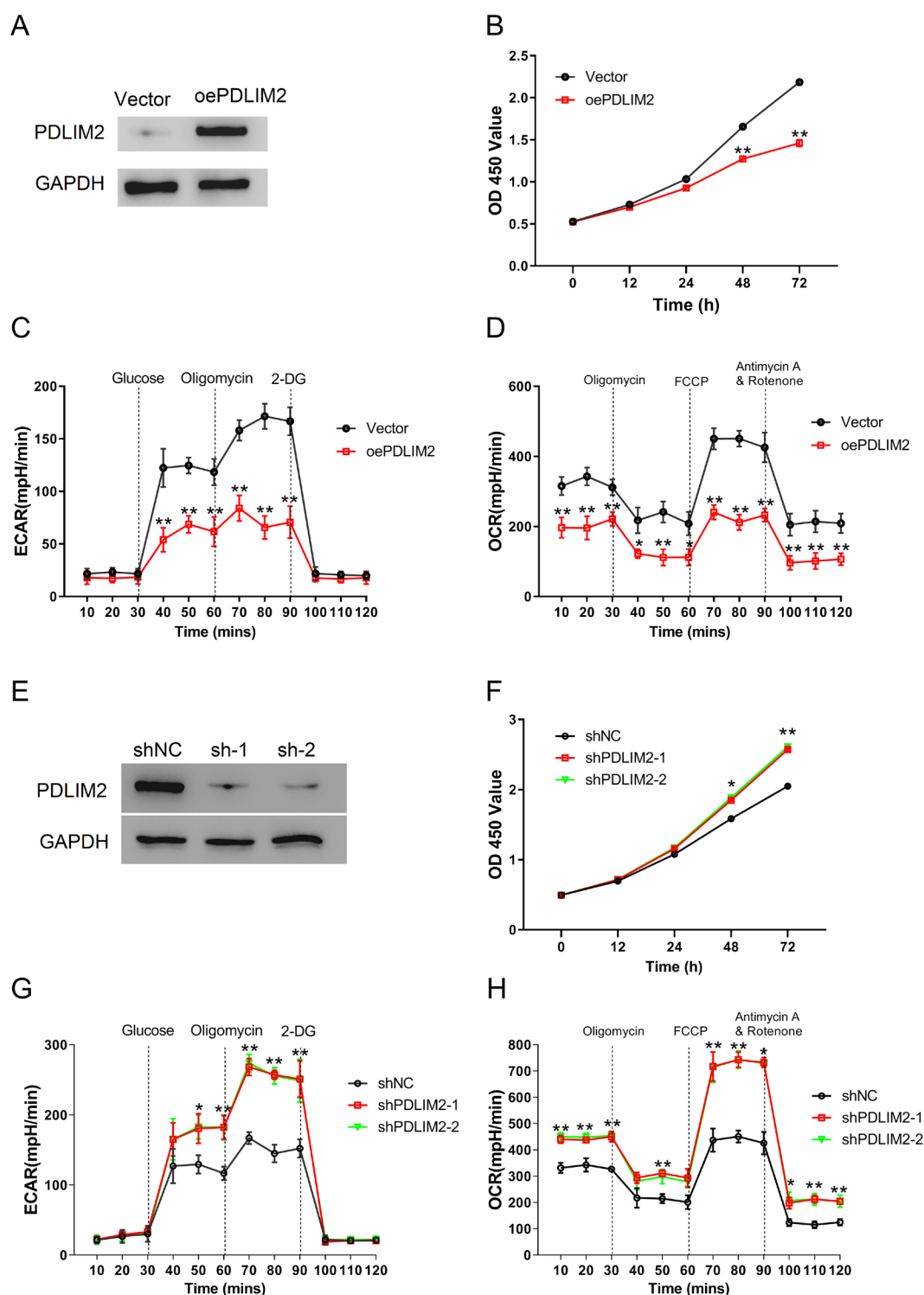
Figure 2. PDLIM2 inhibits proliferation and aerobic glycolysis in FaDu cells. A) Western blot showed efficient overexpression of PDLIM2 by stable transfection in FaDu cells. **B)** CCK-8 assay showed enhanced proliferation of FaDu cells with the overexpression of PDLIM2. **C)** ECAR of Seahorse analysis indicated inhibited glycolysis in FaDu cells with overexpression of PDLIM2. **D)** OCR of the Seahorse analysis indicated reduced oxidative phosphorylation in FaDu cells with over-expression of PDLIM2. **E)** Western blot showed efficient depletion of PDLIM2 by stable transfection of shRNA for RNAi in FaDu cells. **F)** CCK-8 assay showed reduced proliferation of FaDu cells with RNAi knockdown of PDLIM2. **G)** ECAR of Seahorse analysis indicated increased glycolysis in FaDu cells with RNAi knockdown of PDLIM2. **H)** OCR of Seahorse analysis indicated increased oxidative phosphorylation in FaDu cells with RNAi knockdown of PDLIM2. Data presented as mean ± S.D., n = 3, *p<0.05, **p<0.01 (Student's t-test for B–D, and ANOVA for F–H).

suppresses glycolysis, oxidative phosphorylation, and proliferation in LSCC cells.

PDLIM2 promotes PFKL degradation through the ubiquitin-proteasome pathway in FaDu cells. As PDLIM2 was confirmed to be involved in FaDu cell proliferation and glycolysis, we attempted to determine the substrate of this E3 ligase in FaDu cells, which could be a critical downstream effector in these cells. The targets of PDLIM2 were predicted by the Ubibrowser database [18], among which PFKL attracted our attention (Supplementary Figure S1) because it has been reported to promote glycolysis and tumorigenesis in HCC [7]. In FaDu cells, we found that the overexpression of PDLIM2 significantly reduced the protein level of PFKL, while the RNAi knock-down of PDLIM2 enhanced its abundance (Figure 3A). The response of PFKL abundance to altered PDLIM2 level was consistent with the observation that PDLIM2 inhibited glycolysis in FaDu cells. Interestingly, the mRNA expression level of PFKL was not regulated by PDLIM2 as determined by qPCR in FaDu cells with overexpression or knock-down of PDLIM2 (Figure 3A), therefore, it is reasonable to speculate that PFKL expression was very likely to be regulated by PDLIM2 for turnover via the ubiquitin-proteasome pathway, considering the previously reported E3 ubiquitin ligase activity of PDLIM2. Supporting the notion that PDLIM2 promotes degradation of PFKL, these two proteins interact with each other in FaDu cells, confirmed by co-immunoprecipation assay (Figure 3B). Also, the reduction of PFKL abundance in PDLIM2-overexpressing FaDu cells was restored in these cells treated with MG132, the inhibitor of proteasome (Figure 3C), demonstrating that the inhibitory effect of PDLIM2 on PFKL expression was dependent on the ubiquitin-proteasome pathway. Consistently, a higher level of ubiquitination was observed in immunoprecipitated PFKL from PDLIM2-overexpressing FaDu cells, compared with control cells (Figure 3D). These results demonstrated that the PDLIM2 suppressed PFKL expression by promoting its degradation via the ubiquitin-proteasome pathway.

Exosomes from M2 macrophages accelerate proliferation and aerobic glycolysis in FaDu cells by inhibiting the PDLIM2 expression. Considering the close interaction between M2-polarized macrophages and tumors, as well as the broad biological effects of exosomes from M2 macrophages, we directed our attention to the activity of exosomes
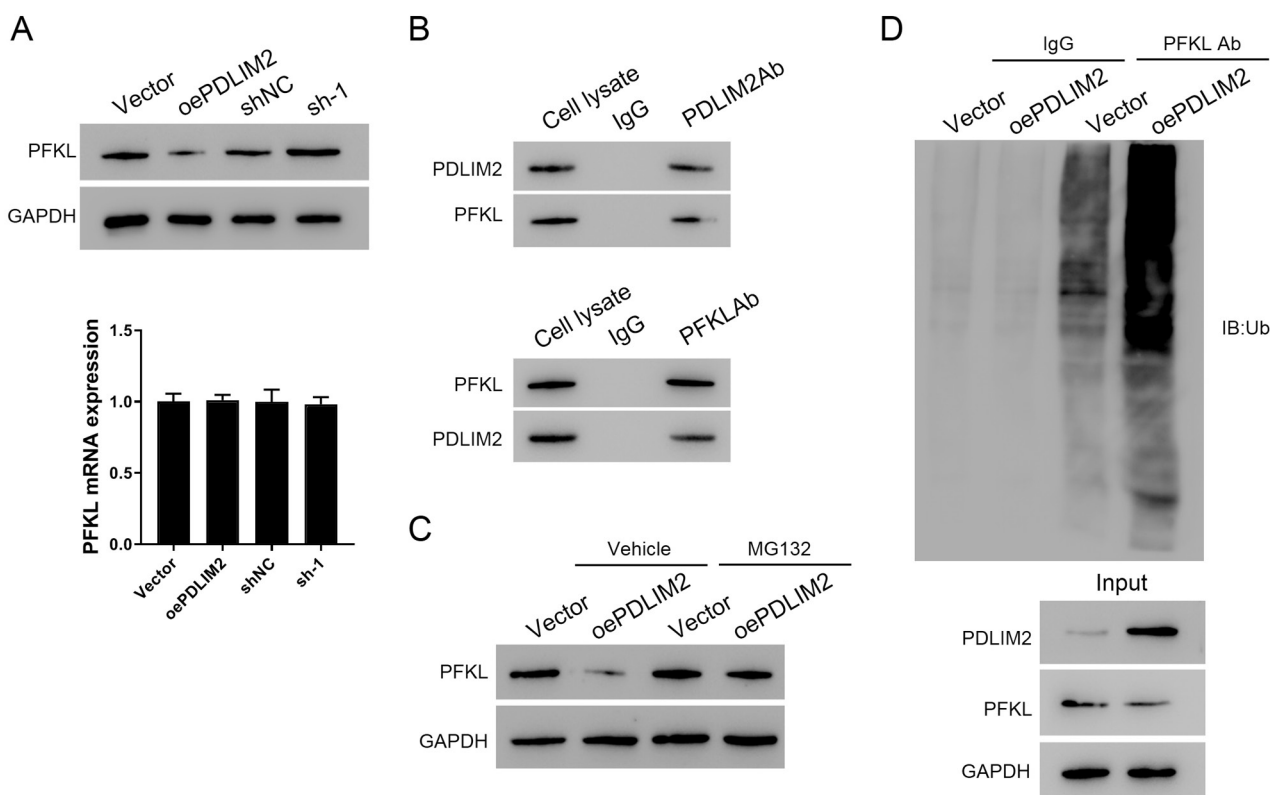

Figure 3. PDLIM2 promotes PFKL degradation through the ubiquitination-proteasome pathway in FaDu cells. A) Western blot determined the reduced or elevated level of PFKL expression in FaDu cells with overexpression or RNAi knockdown of PDLIM2 respectively (upper). The qPCR test found no difference in mRNA level of PFKL in these cells (lower). Data presented as mean ± S.D. B) Co-immunoprecipitation assay to determine the interaction between PDLIM2 and PFKL in FaDu cells. IP PDLIM2 detected PFKL (upper), and IP PFKL detected PDLIM2 (lower). C) Western blot showed that MG132 treatment prevented the downregulation of PFKL by PDLIM2 overexpression. D) Western blot for Ubiquitin in PFKL IP sample showed that the overexpression of PDLIM2 significantly increased Ubiquitin chain ligation to PFKL.

from M2 macrophages in PDLIM2 expression in LSCC tumors. THP-1 human monocyte cell line was cultured and induced to polarize to M2-type (Supplementary Figure S2), and the exosomes secreted from these cells were successfully extracted (Supplementary Figures S3, S4). Echoing previous studies indicating the critical role of exosomes in regulating gene expression in target cells, the culture medium from M2-polarized THP-1 macrophages strongly reduced mRNA and protein expression of PDLIM2 in FaDu cells, while the culture medium from M2-polarized THP-1 macrophages treated by GW4869, the neutral sphingomyelinase inhibitor that extensively blocks exosome secretion, exhibited no effect (Figure 4A). In keeping with this result, the extracted exosomes from the culture medium of M2-polarized THP-1 macrophages strongly inhibited the expression of PDLIM2. This effect was observed at both protein and mRNA levels and showed obvious concentration-dependency (Figure 4B). In accord with the tumor-suppressing role of PDLIM2, treatment with exosomes from the culture medium of M2-polarized THP-1 macrophages remarkably accelerated FaDu cell proliferation. In contrast, these exosomes showed no effect on FaDu cells with the overexpression of PDLIM2 (Figure 4C). By OCR test with the Seahorse analyzer, exosomes from M2-polarized THP-1 macrophages promoted oxidative phosphorylation of control, but not that of PDLIM2-overexpressing FaDu cells (Figure 4D). Similarly, the ECAR test with the Seahorse analyzer found that these exosomes promoted glycolysis of control, but not that of PDLIM2-overexpressing

FaDu cells (Figure 4E). The results described in this part all indicated that LSCC tumor-associated M2 macrophages secreted exosomes to accelerate proliferation and aerobic glycolysis of tumor cells by suppressing PDLIM2 expression.

miR-222-3p mediates the effects of exosomes from M2 macrophages on proliferation and aerobic glycolysis in FaDu cells. It was evidenced that a large proportion of miRNAs showed differential expression in M2- vs. M0-type macrophages [19]. Among them, miR-222-3p, miR-500a-5p, and miR-378a-3p were examined in exosomes extracted from the culture medium of M0- and M2-polarized THP-1 macrophages, which showed the upregulation of miR-222-3p and miR-500a-5p, and downregulation of miR-378a-3p in M2-exosomes (Figure 5A). In contrast, expression of miR-125b-5p, miR-193b-3p, miR-502-3p, and miR-99a-5p exhibited similar level between M0- and M2-exosomes (Supplementary Figure S5).

During the course of analyzing these miRNAs, we noted the potential role of miR-222-3p in PDLIM2 expression. Target prediction of miR-222-3p by the miRWalk database [20] indicated that this miRNA might recognize 3'UTR of PDLIM2 mRNA to suppress PDLIM2 expression (Figure 5B). Therefore, we ectopically expressed miR-222-3p-inhibitor and miR-222-3p-mimic in FaDu cells, and detected expression of PDLIM2. The miR-222-3p-inhibitor strongly increased, while miR-222-3p-inhibitor strongly suppressed PDLIM2 expression at both mRNA (Figure 5C) and protein (Figure 5D) levels. These results were supported by luciferase
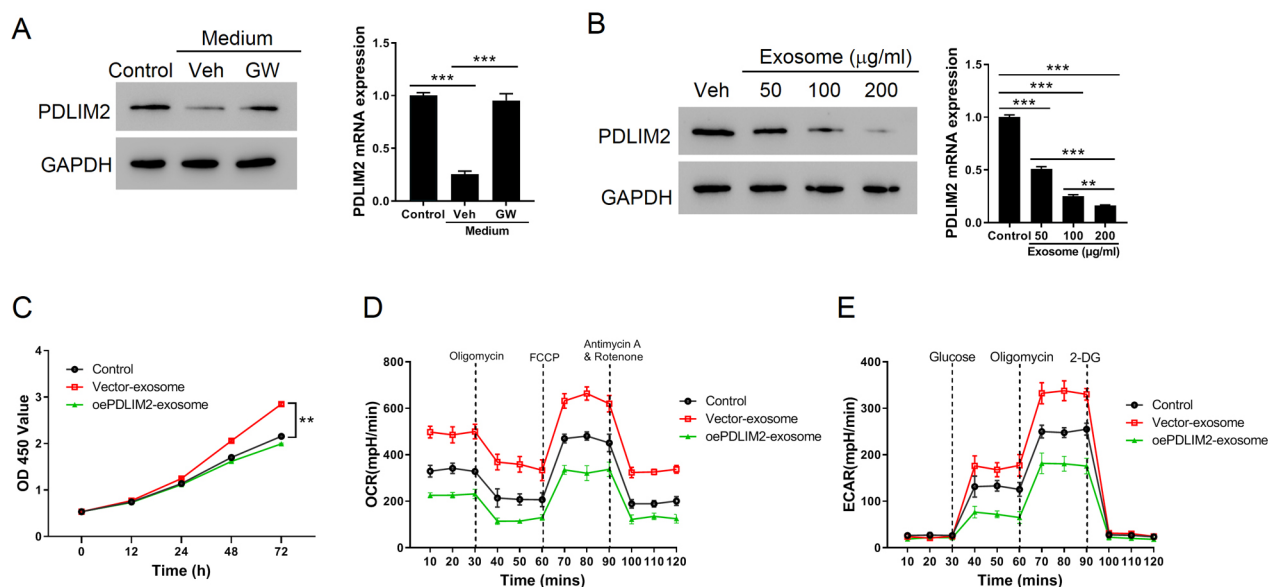

Figure 4. Exosomes from M2 macrophages inhibit PDLIM2 expression to accelerate proliferation and aerobic glycolysis in FaDu cells. A) Western blot (left) and qPCR (right) showed that culture medium of M2 THP-1 macrophages reduced PDLIM2 expression in FaDu cells, while GW4869-treated culture medium had no effect. B) Western blot (left) and qPCR (right) showed that exosomes from M2 THP-1 macrophages inhibited the PDLIM2 expression in FaDu cells. C) CCK-8 assay showed enhanced proliferation of control but not PDLIM2-overexpressing FaDu cells treated with exosomes from M2 THP-1 macrophages. D) OCR test showed increased oxidative phosphorylation of control but not PDLIM2-overexpressing FaDu cells treated with exosomes from M2 THP-1 macrophages. E) ECAR test showed up-regulated glycolysis of control, but not PDLIM2-over-expressing, FaDu cells treated with exosomes from M2 THP-1 macrophages. Data presented as mean ± S.D., n = 3, **p<0.01. ***p<0.001 (ANOVA).

reporter assay, that the reporter harboring miR-222-3p target sequence exhibited increased signal with miR-222-3p-inhibitor and reduced signal with miR-222-3p-mimic, while the reporter containing mutated miR-222-3p target sequence exhibited no change with miR-222-3p-inhibitor or miR-222-3p-mimic (Figure 5E).

To determine if miR-222-3p mediates the effects of M2-exosomes on FaDu cells, miR-222-3p-inhibitor was ectopically expressed. In these cells, compared with control FaDu cells, M2-exosomes could no longer reduce PDLIM2 expression (Figure 5F). Consistently, FaDu cells expressing miR-222-3p-inhibitor only showed mildly enhanced proliferation by treatment of M2-exosomes, compared with the much more dramatic increase in control FaDu cells (Figure 5G). Seahorse metabolic analysis also indicated that expression of miR-222-3p-inhibitor in FaDu cells obviously attenuated the effects of M2-exosomes on activating glycolysis (shown by the ECAR test) and oxidative phosphorylation (shown by the OCR test) (Figure 5H). These observations provided strong support for the notion that exosomes from M2 macrophages employ miR-222-3p to activate proliferation and aerobic glycolysis in LSCC cells through the PDLIM2 inhibition.

Exosomes from M2 macrophages promoted LSCC growth *in vivo*. In light of the observations that exosomes from M2 macrophages activated proliferation and aerobic glycolysis in LSCC cells through PDLIM2 inhibition, we attempted to determine the effects of M2-exosomes on LSCC tumor growth *in vivo*. Subcutaneous injection of FaDu cells into female athymic nude mice resulted in tumor formation. Treatment with M2-exosomes increased the growth rate of tumors. Injection of FaDu cells with overexpression of PDLIM2 failed to form tumors as efficiently as normal FaDu cells, and M2-exosomes could not induce strong tumor growth of these PDLIM2-overexpressing FaDu cells (Figures 6A–6C). Consistently with findings from cell culture experiments, M2-exosomes significantly reduced PDLIM2 expression in tumors formed from FaDu cells, while increased PFKL expression. However, the tumors formed from PDLIM2-overexpressing cells did not show obvious upregulation of PFKL by M2-exosomes treatment (Figure 6D). Therefore, the *in vivo* model supported the tumor-promoting role of M2-exosomes in LSCC.

Discussion

It is now universally appreciated that aerobic glycolysis and tumor-associated M2-type macrophages play essential roles in tumor progression. To test if these mechanisms were at play in the context of LSCC, one of the most prevalent malignant diseases worldwide, we employed a cultured FaDu cell line and conducted a series of functional assays on cell proliferation, mitochondrial metabolism, and also verified the findings from cultured cell-based studies in mice model. Our results further our knowledge of the tumor-promoting role of exosomes of M2 macrophages and aerobic glycolysis

in LSCC etiology, and by elucidating the molecular axis of miR-222-3p/PDLIM2/PFKL, our study identified the mechanistic link for macrophage exosomes, glycolysis, and tumor progression.

As a central member of the family of PDZ and LIM domains-containing proteins, PDLIM2 plays indispensable roles in cell cytoskeleton, polarization, and differentiation. Recently, its involvement in various kinds of cancer was reported [17]. Analyzing the Cancer Genome Atlas and Genotype database, it was found that PDLIM2 was significantly associated with the prognosis of multiple types of cancers. An elevated level of PDLIM2 expression was significantly correlated with tumor grade, and also positively correlated with infiltration of immune cells, supporting its putative role in immune regulation in cancer [21]. Consistently, possibly through inhibiting NF-κB/RelA and STAT3 signals [22], PDLIM2 upregulates genes involved in antigen presentation and activation of T lymphocytes, thereby rendering lung cancer cells vulnerable to anti-PD-1/PD-L1 immune therapy [23]. The function of PDLIM2 in metastasis of kidney cancer was also reported, which was evidenced by both cell culture and animal studies [24]. Our findings further the understanding of PDLIM2 in human cancers where glycolysis becomes an important target of PDLIM2 regulation in LSCC.

With extensive reprogramming of metabolic pathways supporting cell survival and growth, cancer cells always exhibit preferential dependence on glycolysis (relative to oxidative phosphorylation) for energy production in an oxygen-independent manner. This is called the Warburg effect and plays a critical role in tumorigenesis [5]. Although the glycolysis pathway is obviously less efficient than oxidative phosphorylation, regarding the yield of ATP, cancer cells overcome this disadvantage by increasing the glucose uptake. In addition to fueling cellular energy, the metabolic intermediates of glycolysis also serve as a resource for the biosynthesis of various kinds of bio-macromolecules, particularly under conditions with diminished nutrient supply [25]. The progression of LSCC tumor strongly relies on the Warburg effect. The expression of glycolysis-related genes is associated with overall survival in LSCC [26]. Key enzymes in glycolysis actively participate in the pathogenesis of LSCC and could be used as a marker of metastasis, grades, differentiation status, and prognosis. For example, Spindle and kinetochore-associated complex subunit 3 (SKA3) was identified as an oncogene in LSCC, where it could bind with and stabilize the polo-like kinase 1 (PLK1) protein via attenuating its turnover by the ubiquitin-mediated degradation pathway. Consequently, accumulating PLK1 could enable the AKT activation and thus increase the expression of glycolytic enzymes, HK2, PFKFB3, and PDK1, leading to the over-activation of glycolysis in LSCC cells [27]. The miR-125b-5p was significantly downregulated in LSCC. The miR-125b-5p can target and suppress the expression of hexokinase-2 (HK2), a key enzyme functioning in glycolysis, in LSCC cells. This mecha-
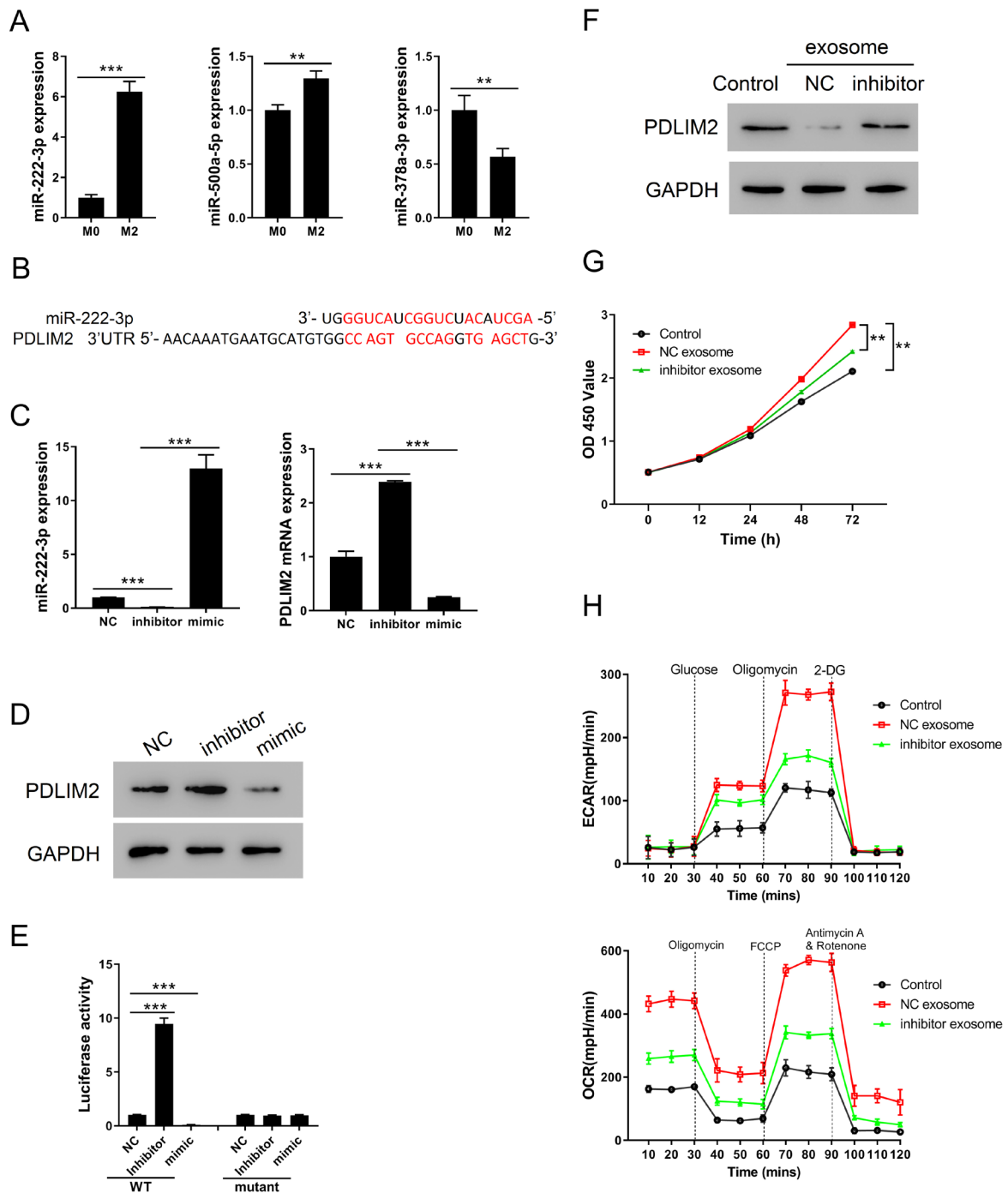
Figure 5. miR-222-3p mediates the effects of exosomes from M2 macrophages on proliferation and aerobic glycolysis in FaDu cells. A) qPCR detection found altered expression of miR-222-3p, miR-500-5p, and miR-378a-3p in M2- vs. M0-exosomes. B) Target prediction found the matched sequences between 3'UTR of PDLIM2 and miR-222-3p. C) qPCR detection confirmed down- and upregulation of miR-222-3p in FaDu cells with miR-222-3p-inhibitor and miR-222-3p-mimic expression, respectively (left). PDLIM2 expression showed up- and downregulation in these cells detected by qPCR (right). D) Western blot showed up- and downregulation of PDLIM2 expression in FaDu cells with miR-222-3p-inhibitor and miR-222-3p-mimic expression, respectively. E) Luciferase reporter assay showed that the reporter harboring miR-222-3p target sequence was activated by miR-222-3p-inhibitor and suppressed by miR-222-3p-mimic, taking the reporter containing mutated miR-222-3p target sequence as control. F) Western blot showed that M2-exosomes reduced expression of PDLIM2, while expression of miR-222-3p-inhibitor restored this reduction. G) CCK-8 assay showed that M2-exosomes enhanced proliferation of FaDu cells, while expression of miR-222-3p-inhibitor partially blocked this effect. H) ECAR test (upper) showed that M2-exosomes promoted glycolysis of FaDu cells, while expression of miR-222-3p-inhibitor partially blocked this effect. OCR test (lower) showed that M2-exosomes promoted oxidative phosphorylation of FaDu cells, while expression of miR-222-3p-inhibitor partially blocked this effect. Data presented as mean ± S.D., n=3, **p<0.01. ***p<0.001 (Student's t-test for A, and ANOVA for G).
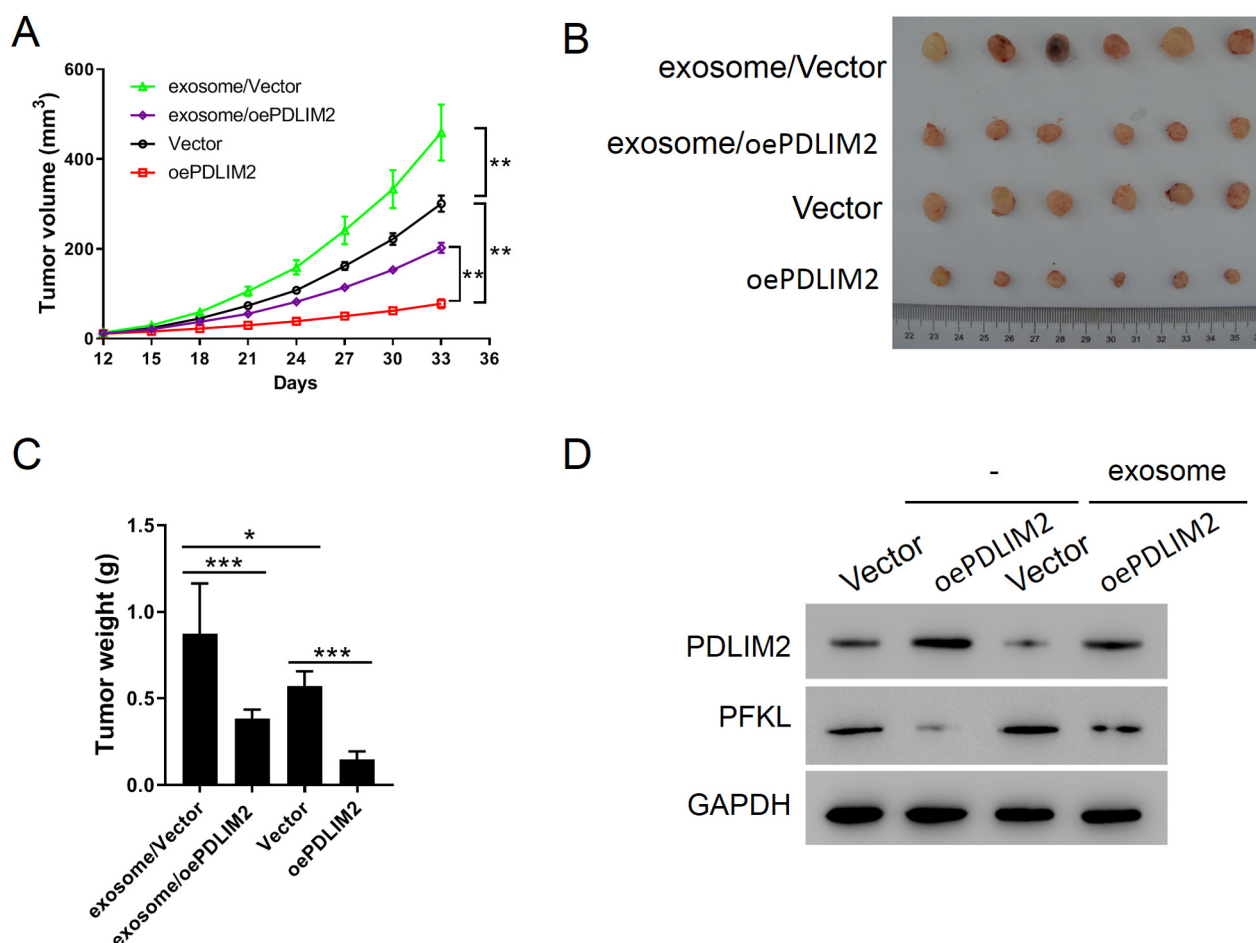
Figure 6. Exosomes from M2 macrophages promoted LSCC growth *in vivo*. A–C) Control or PDLIM2-over-expressing FaDu cells pre-treated with M2-exosomes were injected subcutaneously into nude mice. The enhancement of tumor growth by exosomes and suppression of tumor growth by PDLIM2 overexpression was observed. A) *In vivo* tumor volume, B) measurement of tumor size after sacrificing the mice, C) measurement of tumor weight after sacrificing the mice. D) Western blot showed the reduction of PDLIM2 expression and increase of PFKL expression by M2-exosomes in control FaDu cells, while the PFKL did not show obvious upregulation in PDLIM2-overexpressing FaDu cells. Data presented as mean ± S.D., n=3, *p<0.05, **p<0.01. ***p<0.001 (ANOVA).

nism is indispensable for the tumor-suppressing role of miR-125-5p in LSCC [28]. The long nonprotein coding RNA ferritin heavy chain 1 pseudogene 3 (FTH1P3) plays a crucial role in LSCC pathogenesis. Mechanically, FTH1P3 promoted LDHA enzyme expression by suppressing miR-377-3p, and LDHA largely facilitated LSCC cell glycolysis [29]. Drawing a parallel from these recent findings, our present study unraveled the functional importance of PFKL, an isoform of rate-limiting enzyme (PFK) of glycolysis, in LSCC tumorigenesis, and identified its upstream regulation by E3 ubiquitin ligase (PDLIM2) and miRNA (miR-222-3p). Our study further involved TAMs and their exosomes as initial factors for the miR-222-3p/PDLIM2/PFKL axis, shedding light on the immune cell-tumor communication in LSCC.

Increasing evidence underscores the importance of M2-type macrophages in promoting tumor progression [8].

In LSCC, the number of M2 macrophages was increased and was correlated with a poor prognosis. TGF-β/Smad3 signaling promoted M2 differentiation of TAMs, and JAK/STAT signaling facilitated these M2 macrophages to produce IL-10, which stimulated PD-L1 expression in LSCC tumor cells, leading to its immunosuppression. Taking TGF-β and IL-10 as the targets for therapeutic consideration indicated that these two cytokines synergistically enhance the chemotherapy sensitivity of LSCC tumors [9]. Another report indicated the wide distribution of CD68⁺ TAMs in LSCC and they are positively correlated with CD34-microvascular density (MVD), indicating the essential role these TAMs play in angiogenesis and metastasis [10]. A more specific mechanistic study found that HMGB1 promotes lymphangiogenesis by activation of Receptor for advanced glycation end products (RAGE) on M2 macrophages, which could be

involved in lymph node metastasis and a poor prognosis of LSCC [30]. These results triggered our interest in exploring the function of M2-type macrophages in LSCC, and our findings confirmed their essential roles in LSCC as the factory of tumor-promoting exosomes.

Exosomes become an attractive focus of cancer research recently [11]. The exosomes are extracellular vesicles (EVs) originating from endosomes, with diameters ranging between 30 and 150 nm, and are frequently detected in the urine, blood, and other samples of cerebrospinal fluid [11]. Exosomes could carry cargoes containing multiple cellular components, such as proteins, lipids, DNAs, transposable elements, and RNAs (either coding or non-coding). These cargos are released as exosomes and delivered to target cells [12]. In LSCC, cancer-associated fibroblasts (CAF) release exosomes with aberrant expression of miRNAs. The miRNAs with top abundance could target genes involved in tumor microenvironment remodeling and act as biomarkers for LSCC intervention [31]. A more detailed study identified that miR-941 carried by LSCC serum exosomes could serve as an oncogenic biomarker for diagnosing LSCC, and its action to promote cell proliferation and invasion was also observed for cultured LSCC cells [32]. The present study detected exosomes from M2 macrophages in the LSCC microenvironment and revealed that these exosomes similarly enable tumor cell growth and accelerate glycolysis via suppressing PDLIM2 in target cells. Moreover, a previous study has shown a large proportion of miRNAs showing differential expression in M2- vs. M0-type macrophages [19]. Here, we found that miR-222-3p, which potentially targeted PDLIM2, was elevated in M2-exosomes. It has been reported that miR-222b-3p was significantly upregulated in LSCC, and significantly related to positive family history [33]. Additionally, studies have shown that miR-222-3p can target various potential target genes to regulate cancer cell functions, such as PUMA in non-small cell lung cancer cells [34], and GNAI2 in epithelial ovarian cancer (EOC) cells [35]. However, the specific role of miR-222-3p in LSCC is unclear. The results of the current study suggested that M2-exosomes accelerated LSCC cell proliferation and glycolysis via delivering miR-222-3p to target cells, and miR-222-3p may act as an upstream mediator for PDLIM2. miR-214 [36] and miR-221 [37], which are highly homologous to miR-222-3p, have been reported to target PDLIM2. miR-221-3p was enriched in M2 macrophages of EOC patients and contributed to the proliferation and G1/S transition of EOC cells by targeting CDKN1B [38]. Whether miR-221-3p or miR-214 is enriched in M2-type macrophages, and whether they function in LSCC cells need to be clarified in the future.

Overall, the findings presented here echo previous reports emphasizing the central roles of TAMs, their exosomes and aerobic glycolysis in tumorigenesis, and the action of the molecular axis of miR-222-3p/PDLIM2/PFKL not only provides a blueprint to understand the mechanistic link of TAM exosomes and glycolysis in LSCC but also contribute to the future development of LSCC therapeutic strategies targeting specific molecular pathways.

Supplementary information is available in the online version of the paper.

References

[1]   MARIONI G, MARCHESE-RAGONA R, CARTEI G, MARCHESE F, STAFFIERI A. Current opinion in diagnosis and treatment of laryngeal carcinoma. Cancer Treat Rev 2006; 32: 504–515. https://doi.org/10.1016/j.ctrv.2006.07.002

[2]   FORASTIERE AA, TROTTI A, PFISTER DG, GRANDIS JR. Head and neck cancer: recent advances and new standards of care. J Clin Oncol 2006; 24: 2603–2605. https://doi.org/10.1200/JCO.2006.07.1464

[3]   BURR AR, HARARI PM, HAASL AM, WIELAND AM, BRUCE JY et al. Clinical outcomes for larynx patients with cancer treated with refinement of high-dose radiation treatment volumes. Head Neck 2020; 42: 1874–1881. https://doi.org/10.1002/hed.26098.

[4]   MARIONI G, MARCHESE-RAGONA R, KLEINSASSER NH, LIONELLO M, LAWSON G et al. Partial laryngeal surgery in recurrent carcinoma. Acta Otolaryngol 2015; 135: 119–124. https://doi.org/10.3109/00016489.2014.969811

[5]   YUAN Y, LI H, PU W, CHEN L, GUO D et al. Cancer metabolism and tumor microenvironment: fostering each other? Sci China Life Sci 2022; 65: 236–279. https://doi.org/10.1007/s11427-021-1999-2

[6]   ZUO J, TANG J, LU M, ZHOU Z, LI Y et al. Glycolysis Rate-Limiting Enzymes: Novel Potential Regulators of Rheumatoid Arthritis Pathogenesis. Front Immunol 2021; 12: 779787. https://doi.org/10.3389/fimmu.2021.779787

[7]   FENG Y, ZHANG Y, CAI Y, LIU R, LU M et al. A20 targets PFKL and glycolysis to inhibit the progression of hepatocellular carcinoma. Cell Death Dis 2020; 11: 89. https://doi.org/10.1038/s41419-020-2278-6

[8]   WU D, LIU X, MU J, YANG J, WU F et al. Therapeutic Approaches Targeting Proteins in Tumor-Associated Macrophages and Their Applications in Cancers. Biomolecules 2022; 12: 392. https://doi.org/10.3390/biom12030392

[9]   ZHANG P, ZHANG Y, WANG L, LOU W. Tumor-regulated macrophage type 2 differentiation promotes immunosuppression in laryngeal squamous cell carcinoma. Life Sci 2021; 267: 118798. https://doi.org/10.1016/j.lfs.2020.118798

[10]   SUN S, PAN X, ZHAO L, ZHOU J, WANG H et al. The Expression and Relationship of CD68-Tumor-Associated Macrophages and Microvascular Density With the Prognosis of Patients With Laryngeal Squamous Cell Carcinoma. Clin Exp Otorhinolaryngol 2016; 9: 270–277. https://doi.org/10.21053/ceo.2015.01305

[11] WAQAS MY, JAVID MA, NAZIR MM, NIAZ N, NISAR MF et al. Extracellular vesicles and exosome: insight from physiological regulatory perspectives. J Physiol Biochem 2022. https://doi.org/10.1007/s13105-022-00877-6

[12] TIAN Y, CHENG C, WEI Y, YANG F, LI G. The Role of Exosomes in Inflammatory Diseases and Tumor-Related Inflammation. Cells 2022; 11: 1005. https://doi.org/10.3390/cells11061005

[13] ZHENG P, LUO Q, WANG W, LI J, WANG T et al. Tumor-associated macrophages-derived exosomes promote the migration of gastric cancer cells by transfer of functional Apolipoprotein E. Cell Death Dis 2018; 9: 434. https://doi.org/10.1038/s41419-018-0465-5

[14] BINENBAUM Y, FRIDMAN E, YAARI Z, MILMAN N, SCHROEDER A et al. Transfer of miRNA in Macrophage-Derived Exosomes Induces Drug Resistance in Pancreatic Adenocarcinoma. Cancer Res 2018; 78: 5287–5299. https://doi.org/10.1158/0008-5472.CAN-18-0124

[15] YANG M, CHEN J, SU F, YU B, SU F et al. Microvesicles secreted by macrophages shuttle invasion-potentiating microRNAs into breast cancer cells. Mol Cancer 2011; 10: 117. https://doi.org/10.1186/1476-4598-10-117

[16] LAN J, SUN L, XU F, LIU L, HU F et al. M2 Macrophage-Derived Exosomes Promote Cell Migration and Invasion in Colon Cancer. Cancer Res 2019; 79: 146–158. https://doi.org/10.1158/0008-5472.CAN-18-0014

[17] GUO Z, SQU Z. PDLIM2: Signaling pathways and functions in cancer suppression and host immunity. Biochim Biophys Acta Rev Cancer 2021; 1876: 188630. https://doi.org/10.1016/j.bbcan.2021.188630

[18] LI Y, XIE P, LU L, WANG J, DIAO L et al. An integrated bioinformatics platform for investigating the human E3 ubiquitin ligase-substrate interaction network. Nature communications 2017; 8: 347. https://doi.org/10.1038/s41467-017-00299-9

[19] COBOS JIMENEZ V, BRADLEY EJ, WILLEMSEN AM, VAN KAMPEN AH, BAAS F et al. Next-generation sequencing of microRNAs uncovers expression signatures in polarized macrophages. Physiol Genomics 2014; 46: 91–103. https://doi.org/10.1152/physiolgenomics.00140.2013

[20] STICHT C, DE LA TORRE C, PARVEEN A, GRETZ N. miRWalk: An online resource for prediction of microRNA binding sites. PloS One 2018; 13: e0206239. https://doi.org/10.1371/journal.pone.0206239

[21] ZENG Y, LIN D, GAO M, DU G, CAI Y. Systematic evaluation of the prognostic and immunological role of PDLIM2 across 33 cancer types. Sci Rep 2022; 12: 1933. https://doi.org/10.1038/s41598-022-05987-1

[22] SHI H, JI Y, LI W, ZHONG Y, MING Z. PDLIM2 acts as a cancer suppressor gene in non-small cell lung cancer via the down regulation of NF-kappaB signaling. Mol Cell Probes 2020; 53: 101628. https://doi.org/10.1016/j.mcp.2020.101628

[23] SUN F, LI L, YAN P, ZHOU J, SHAPIRO SD et al. Causative role of PDLIM2 epigenetic repression in lung cancer and therapeutic resistance. Nat Commun 2019; 10: 5324. https://doi.org/10.1038/s41467-019-13331-x

[24] YUK HD, LEE KH, LEE HS, JEONG SH, KHO Y et al. PDLIM2 Suppression Inhibit Proliferation and Metastasis in Kidney Cancer. Cancers (Basel) 2021; 13: 2991. https://doi.org/10.3390/cancers13122991

[25] KOZAL K, JOZWIAK P, KRZESLAK A. Contemporary Perspectives on the Warburg Effect Inhibition in Cancer Therapy. Cancer Control 2021; 28: 10732748211041243. https://doi.org/10.1177/10732748211041243

[26] LAU HC, SHEN Y, HUANG Q, HUANG H Y, ZHOU L. Glycolysis related gene expression signature in predicting prognosis of laryngeal squamous cell carcinoma. Bioengineered 2021; 12: 8738–8752. https://doi.org/10.1080/21655979.2021.1980177

[27] GAO W, ZHANG Y, LUO H, NIU M, ZHENG X et al. Targeting SKA3 suppresses the proliferation and chemoresistance of laryngeal squamous cell carcinoma via impairing PLK1-AKT axis-mediated glycolysis. Cell Death Dis 2020; 11: 919. https://doi.org/10.1038/s41419-020-03104-6

[28] HUI L, ZHANG J, GUO X. MiR-125b-5p suppressed the glycolysis of laryngeal squamous cell carcinoma by down-regulating hexokinase-2. Biomed Pharmacother 2018; 103: 1194–1201. https://doi.org/10.1016/j.biopha.2018.04.098

[29] ZHAO L, ZHENG Y, ZHANG L, SU L. E2F1-Induced FTH1P3 Promoted Cell Viability and Glycolysis Through miR-377-3p/LDHA Axis in Laryngeal Squamous Cell Carcinoma. Cancer Biother Radiopharm 2022; 37: 276–286. https://doi.org/10.1089/cbr.2020.4266

[30] SU C, JIA S, MA Z, ZHANG H, WEI L et al. HMGB1 Promotes Lymphangiogenesis through the Activation of RAGE on M2 Macrophages in Laryngeal Squamous Cell Carcinoma. Dis Markers 2022; 2022: 4487435. https://doi.org/10.1155/2022/4487435

[31] WU C, WANG M, HUANG Q, GUO Y, GONG H et al. Aberrant expression profiles and bioinformatic analysis of CAF-derived exosomal miRNAs from three moderately differentiated supraglottic LSCC patients. J Clin Lab Anal 2022; 36: e24108. https://doi.org/10.1002/jcla.24108

[32] ZHAO Q, ZHENG X, GUO H, XUE X, ZHANG Y et al. Serum Exosomal miR-941 as a promising Oncogenic Biomarker for Laryngeal Squamous Cell Carcinoma. J Cancer 2020; 11: 5329–5344. https://doi.org/10.7150/jca.45394

[33] KYURKCHIYAN SG, POPOV TM, STANCHEVA G, RANGACHEV J, MITEV VI et al. Novel insights into laryngeal squamous cell carcinoma from association study of aberrantly expressed miRNAs, lncRNAs and clinical features in Bulgarian patients. J BUON 2020; 25: 357–366.

[34] CHEN W, LI X. MiR-222-3p promotes cell proliferation and inhibits apoptosis by targeting PUMA (BBC3) in non-small cell lung cancer. Technol Cancer Res Treat 2020; 19: 1533033820922558. https://doi.org/10.1177/1533033820922558

[35] FU X, LI Y, ALVERO A, LI J, WU Q et al. MicroRNA-222-3p/GNAI2/AKT axis inhibits epithelial ovarian cancer cell growth and associates with good overall survival. Oncotarget 2016; 7: 80633. https://doi.org/10.18632/oncotarget.13017

[36] POLYTARCHOU C, HOMMES DW, PALUMBO T, HATZI-APOSTOLOU M, KOUTSIOUMPAM et al. MicroRNA214 is associated with progression of ulcerative colitis, and inhibition reduces development of colitis and colitis-associated cancer in mice. Gastroenterology 2015; 149: 981–992. e11. https://doi.org/10.1053/j.gastro.2015.05.057

[37] SONG Q, AN Q, NIU B, LU X, ZHANG N et al. Role of miR-221/222 in tumor development and the underlying mechanism. J Oncol 2019; 2019: 7252013. https://doi.org/10.1155/2019/7252013

[38] LI XTANG M. Exosomes released from M2 macrophages transfer miR-221-3p contributed to EOC progression through targeting CDKN1B. Cancer Med 2020; 9: 5976–5988. https://doi.org/10.1002/cam4.3252

Exosomes from M2 macrophages promoted glycolysis in FaDu cells by inhibiting PDLIM2 expression to stabilize PFKL

Peng WANG[1], Guang-Yao LI[1], Lei ZHOU[1], Huai-Li JIANG[1], Yue YANG[2], Hai-Tao WU[2,*]

Supplementary Information

Supplementary Table S1. Primer sequences for real-time PCR.

| Gene	Forward primer	Reverse primer
PDLIM2	5' TGCTACACCTGTGCCGACTG 3'	5' GCAACTGCCCACCATTGTCC 3'
PFKL	5' GGCACAATACCGCATCAG 3'	5' AGGCTCCAGACACAACAG 3'
MRC1	5' TCCTCAGCTCTCCACAATC 3'	5' GTACCTTTGCCCACTTCAC 3'
CCL13	5' CACACCCTGAAGACTTGAAC 3'	5' GCTTAGAGACAGCAACCTAC 3'
ARG1	5' TCCAGAACCATAGGGATTATTG 3'	5' TTTGAAAGGGACTGTCATTAGG 3'
GAPDH	5' AATCCCATCACCATCTTC 3'	5' AGGCTGTTGTCATACTTC 3'

Supplementary Table S2. Primer sequences for miRNA.

| miRNA	Primers
hsa-miR-222-3p	Primer RT
	5' GTCGTATCCAGTGCAGGGTCCGAGGTATTCGCACTGGATACGACACCCAG 3'
	Primer F: 5' GCGCGAGCTACATCTGGCTA 3'
	Primer R: 5' AGTGCAGGGTCCGAGGTATT 3'
hsa-miR-125b-5p	Primer RT
	5' GTCGTATCCAGTGCAGGGTCCGAGGTATTCGCACTGGATACGACTCACAA 3'
	Primer F: 5' CGCGTCCCTGAGACCCTAAC 3'
	Primer R: 5' AGTGCAGGGTCCGAGGTATT 3'
hsa-miR-193b-3p	Primer RT
	5' GTCGTATCCAGTGCAGGGTCCGAGGTATTCGCACTGGATACGACAGCGGG 3'
	Primer F: 5' GCGAACTGGCCCTCAAAGT 3'
	Primer R: 5' AGTGCAGGGTCCGAGGTATT 3'
hsa-miR-500a-5p	Primer RT
	5' GTCGTATCCAGTGCAGGGTCCGAGGTATTCGCACTGGATACGACTCTCAC 3'
	Primer F: 5' CGCGTAATCCTTGCTACCTGG 3'
	Primer R: 5' AGTGCAGGGTCCGAGGTATT 3'
hsa-miR-502-3p	Primer R
	5' GTCGTATCCAGTGCAGGGTCCGAGGTATTCGCACTGGATACGACTGAATC 3'
	Primer F: 5' CGAATGCACCTGGGCAAG 3'
	Primer R: 5' AGTGCAGGGTCCGAGGTATT 3'
hsa-miR-378a-3p	Primer RT
	5' GTCGTATCCAGTGCAGGGTCCGAGGTATTCGCACTGGATACGACGCCTTC 3'
	Primer F: 5' CGCGACTGGACTTGGAGTCA 3'
	Primer R: 5' AGTGCAGGGTCCGAGGTATT 3'
hsa-miR-99a-5p	Primer RT
	5' GTCGTATCCAGTGCAGGGTCCGAGGTATTCGCACTGGATACGACCACAAG 3'
	Primer F: 5' GCGAACCCGTAGATCCGAT 3'
	Primer R: 5' AGTGCAGGGTCCGAGGTATT 3'
cel-miR-39-3p	Primer RT
	5' GTCGTATCCAGTGCAGGGTCCGAGGTATTCGCACTGGATACGACCAAGCT 3'
	Primer F: 5' GCGTCACCGGGTGTAAATC 3'
	Primer R: 5' AGTGCAGGGTCCGAGGTATT 3'

Supplementary Table S3. Antibodies list.

| Primary antibody	Company	Catalog No.
PDLIM2	Abcam	ab246868
PFKL	Abcam	Ab241093
TSG101	Abcam	Ab125011
CD63	Abcam	Ab118307
GAPDH	Cell Signaling Technology	#5174
Ubiquitin	Abcam	Ab7780

Known ubiquitination sites and predicted recognizing motif/domain for substrate: PFKL mediated by E3 ligase: PDLIM2
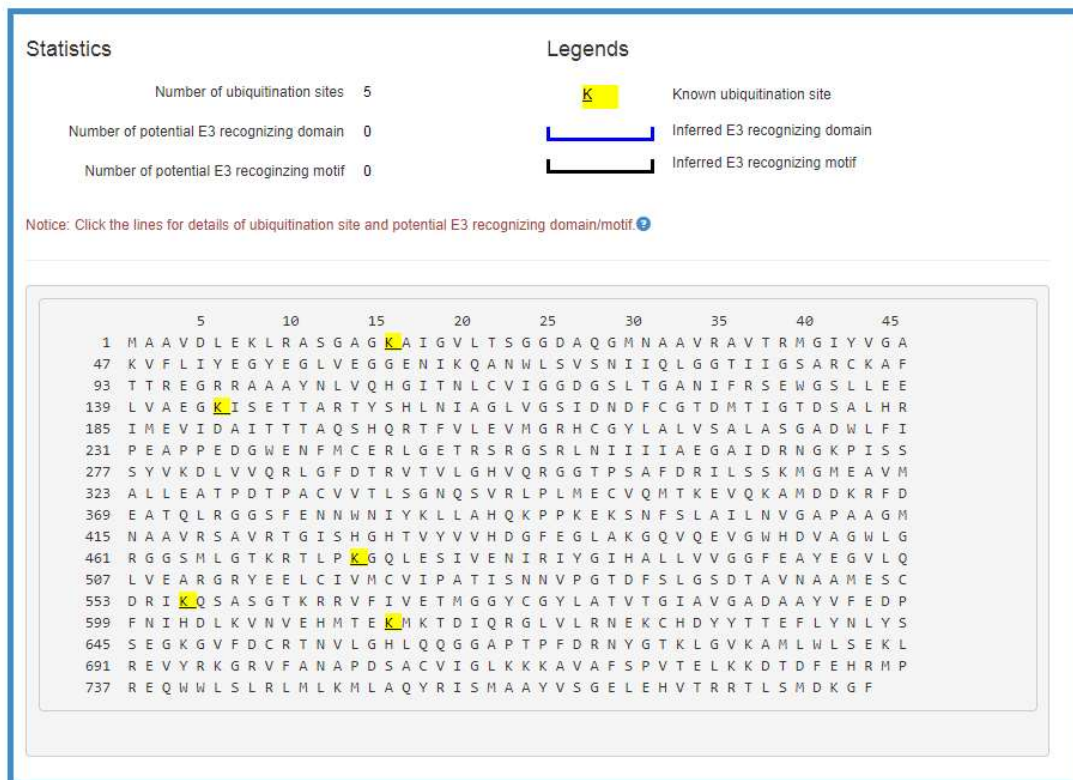
Supplementary Figure S1. Known ubiquitination sites and predicted recognizing motif/domain for PFKL mediated by PDLIM2 (Ubibrowser database).
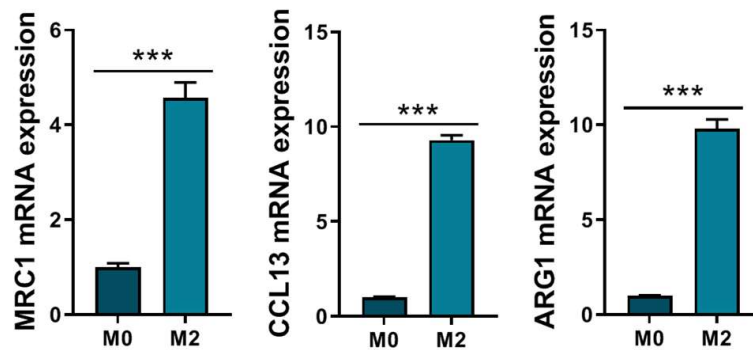

Supplementary Figure S2. M2 differentiation of THP-1 monocyte cell line. The M2 macrophage marker genes were determined by qPCR. Data presented as mean±S.D., n=3, *p<0.05, **p<0.01. ***p<0.001
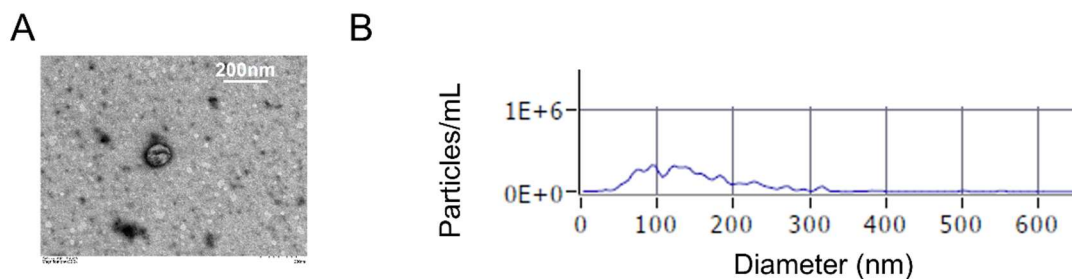
Supplementary Figure S3. Characterization of exosomes extracted from culture medium of differentiated M2 macrophages. A) Representative electron micrograph image. B) Particle size distribution in purified pellets consistent with size range of exosomes (average size 100 nm), measured by ZetaView® Particle Tracking Analyzer.
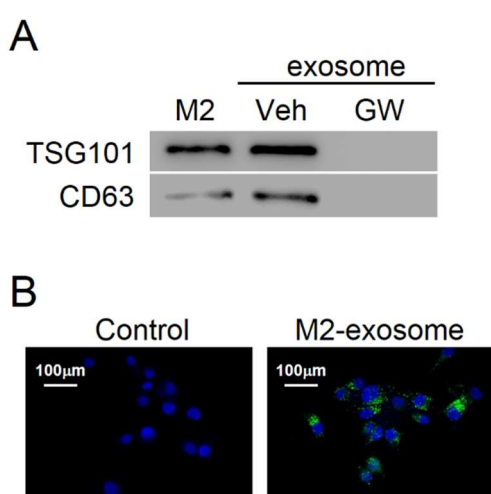
Supplementary Figure S4. Characterization of exosomes produced and secreted from differentiated M2 macrophages. A) Western blot showed the exosome markers, TSG101 and CD63, in M2 macrophages and extracted exosomes, taking GW4869-treated samples as control. B) PKH-67 staining indicated the engulfment of M2 exosomes into FaDu cells.
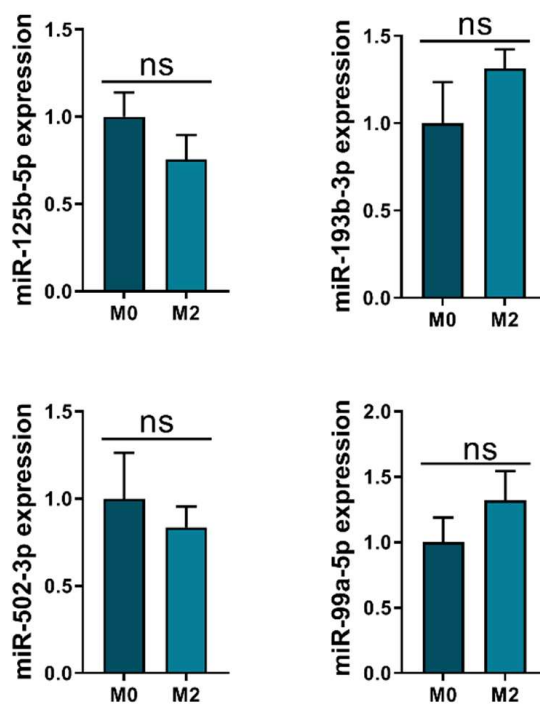
Supplementary Figure S5. Altered expression of miRNAs in M2- Vs M0-exosomes. The qPCR showed expression level of miR-125b-5p, miR-193b-3p, miR-502-3p and miR-99a-5p. Data presented as mean±S.D., n=3, *p<0.05, **p<0.01. ***p<0.001